2017 International Conference on Rehabilitation Robotics (ICORR)
QEII Centre, London, UK, July 17-20, 2017.

Preliminary Study of a Robotic Foot-Ankle Prosthesis with Active Alignment

Andrew K. LaPre, Ryan D. Wedge, Brian R. Umberger, Frank C. Sup IV, *Member, IEEE*

Abstract — **Robotic prosthetic foot-ankle prostheses typically aim to replace the lost joint with revolute joints aimed at replicating normal joint biomechanics. In this paper, a previously developed robotic ankle prosthesis with active alignment is evaluated. It uses a four-bar mechanism to inject positive power into the gait cycle while altering the kinematics of the ankle joint and pylon segment to reduce loading on the residual limb. In a single-subject biomechanics analysis, there was a 10% reduction in peak limb pressures and evidence of greater gait symmetry in ground reaction forces when active alignment was implemented compared to walking with the daily use prosthesis. These results provide preliminary evidence that an alternative lower limb prosthesis may be capable of improving gait characteristics over traditional revolute designs.**

I. Introduction

Following lower limb amputation, a person's gait is a result of their overall health, prosthesis and the connecting interface at the residual limb [1]. High loads borne by soft tissues at this interface [2], [3] are often a source of discomfort [4], [5] and further damage to the limb [6], [7]. These issues can lead to further problems elsewhere in the body [6], [8], [9] and discontinued use of the prosthesis [10]–[12]. Daily activities such as standing and walking can become incredibly challenging [10], [12], [13], causing physical activity levels to decrease which often leads to further deterioration of overall health. Designing a prosthesis to imitate the form and function of the lost limb, without taking interface loading limitations into consideration, may be insufficient for maximally restoring gait and mobility.

Active alignment is a novel design feature in a robotic transtibial prosthesis prototype (Fig. 1) developed by the authors in previous research [14]–[18]. Active alignment utilizes active components and an optimized mechanism to realign the residual limb in relation to the ground reaction force (GRF) during mid to late stance. The prosthesis alignment is continuously adjusted in an effort to reduce both moment transfer to the limb and associated peak pressures on the residual limb, while power is injected into the stride. If the loading demand on the residual limb decreases, it is anticipated that it will help to keep an individual active longer and enable them to maintain their general health.

In this paper, the prosthesis performance and its effect on gait mechanics are evaluated in a comprehensive biomechanics study. The methods are detailed which include the experimental procedures and data post-processing. Results are then presented, covering whole-body biomechanics, ground reaction forces (GRFs), center of mass (COM) trajectories, residuum-socket mechanics, prosthesis performance metrics, and intra-socket pressure recordings during gait. The findings and implications of prosthesis design warrant continued prosthesis development.

II. Methods

A. Experimental Procedures

In this study, a high activity level (K-4) test subject with below-knee amputation was recruited and biomechanics were captured using their own passive energy storage and return (ESR) prosthetic foot and using the active alignment prosthesis (AAP). Approval from the Institutional Review Board at the University of Massachusetts Amherst was obtained for this human subject study. The subject (Table 1) had already walked on the device in three prior experiments, and was comfortable and stable walking on the prototype

Fig. 1. Active alignment is a design feature that realigns the limb towards the center of pressure during stance phase of walking. Active alignment reduces peak moment transfer to the limb, resulting in reduced intra-socket peak pressures.

A. K. LaPrè, Ph.D., is a research scientist at the University of Massachusetts Amherst, MA 01002 USA (e-mail: alapree@umass.edu).

R. D. Wedge is a Ph.D. candidate in the Kinesiology Department at the University of Massachusetts, Amherst MA 01003 USA (e-mail: rwedge@kin.umass.edu).

B. R. Umberger is an Associate Professor in the Kinesiology department at the University of Massachusetts Amherst, MA 01003 USA (phone: 413-545-1436, fax: 413-545-2906, email: umberger@kin.umass.edu)

F.C. Sup IV is an Associate Professor in the Mechanical and Industrial Engineering Department, University of Massachusetts Amherst, MA 01003 USA (corresponding author phone: 413-545-2946; fax: 413-545-1027; e-mail: sup@umass.edu).

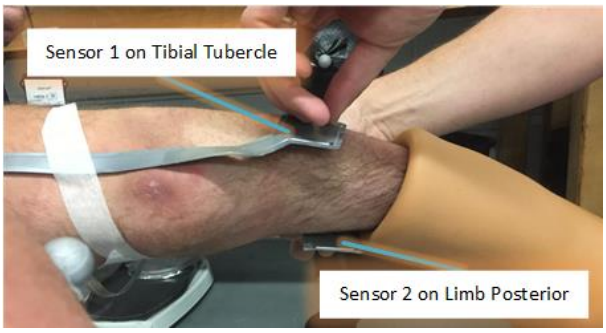

Fig. 2. The subject's residual limb instrumented with Novel Pliance pressure sensors on the tibial tubercle and limb posterior.

without an overhead harness. All testing in this evaluation consisted of steady state walking at the subject's preferred speed while data were collected. Data recorded during this test session included tracking experimental markers attached to the subject's limbs, head and torso through three-dimensional space, recording GRFs, and recording intra-socket pressure on load bearing surfaces of the residual limb. All biomechanics testing took place in the Kinesiology Department Biomechanics Laboratory at the University of Massachusetts Amherst.

Prior to testing, the subject was fitted with infrared reflective tracking markers on the head arms and torso for both model scaling and motion tracking. Scaling markers placed at bony anatomical landmarks consisted of left and right acromion process, iliac crest, anterior superior iliac spine (ASIS), posterior superior iliac spine (PSIS), greater trochanter, lateral and medial femoral condyles, lateral and medial malleoli, first metatarsal head, fifth metatarsal head, and tip of the second toe. Markers on the prosthesis were matched with the intact contralateral limb. Tracking markers included acromion processes, iliac crests, ASISs, PSISs, toes, four marker clusters on the thighs, right shank, and socket, and clusters of three markers on heels of the shoes. The residual limb was also instrumented with 3x4 grid array capacitive pressure transducers on the tibial tubercle and mid posterior region (Fig. 2), connected to a wireless transponder worn on the hip. Measurements of the subject's residual limb were also taken at this time.

During testing, marker trajectories were calculated in real-time via measurements taken from an eleven-camera optical motion capture system (Qualisys, Inc., Gothenberg, Sweden) at 240 Hz, and ground reaction forces were recorded at 2400 Hz using three flush-mounted strain gauge force

TABLE 1. TEST SUBJECT DATA.

Height (m)	1.83
Mass w/ Passive Prosthesis (kg)	73.16
Mass w/ Active Prosthesis (kg)	74.28
Gender	Male
Amputation Level	Left Transtibial
Activity Level	K-4
Daily Use Prosthesis	Ability Dynamics Rush 87
Residual/Intact Limb Ratio	0.59
Preferred Walking Speed (m/s)	1.32

Fig. 3. The subject is shown posing for a static standing calibration trial, where marker positions were used for model scaling during data post processing.

platforms (OR6-5, AMTI, Inc. Watertown, MA, USA) integrated into the Qualysis Track Manager software. The pressure inside the socket was recorded with a Novel Pliance pressure measurement system (Novel, Inc., Munich Germany). A custom radio frequency trigger was designed to synchronize pressure data with marker and GRF data. A wireless signal sent a logic high signal to the data collection board on the first frame to be used during post-processing. Trigger delay was measured to be less than one camera frame.

Prior to experimental trials, static calibration trials were performed to establish scale factors and subject weight (Fig. 3). The subject first stood on the force platform closest to the center of the data collection area in a normal standing pose where all limbs were straight, and arms extended out laterally. Marker and force data were recorded for ten seconds with the subject standing as still as possible. The same protocol was then repeated with the subject standing in a flexed pose where all limbs were slightly bent to better establish joint centers of rotation during scaling.

Test trials for this evaluation consisted of normal walking at the subject's preferred speed. To establish a preferred speed baseline, the subject was tasked to walk through the data collection area five times measuring speed with photogates spaced 6 m apart. After establishing a baseline, the subject performed the same task while wearing their daily use prosthesis while all data were recorded until three successful trials were completed. A successful trial was considered one in which the subject was within 5% of their preferred speed, and struck all three force platforms without targeting. The subject was then outfitted with the active alignment prosthesis and heuristically aligned to match the passive prosthesis based on walking observations, photographs, and subject feedback. The alignment coefficient, described in [17], [18], was heuristically tuned to maximize moment transfer reduction just before toe off and to minimize actuator stall. The optimal coefficient value is dependent on walking style, which varies from subject to

$$C = \sum_{n=1}^{n_{frames}} \sum_{m=1}^{m_{markers}} \sqrt{\left(Mx_{nm} - Ex_{nm}\right)^2 + \left(My_{nm} - Ey_{nm}\right)^2 + \left(Mz_{nm} - Ez_{nm}\right)^2} + \sum_{n=n_{frames}-0.1*n_{frames}}^{n_{frames}} W_1 flex_n \quad (1)$$

subject as well as test conditions (i.e. treadmill vs. overground). After a brief acclimation period and another set of static calibration trials, the subject repeated the walking trials until three successful trials were completed.

B. Data Processing

Two generic musculoskeletal OpenSim models for a person with left transtibial amputation were used, one with a generic passive prosthesis and the other with the modified active alignment prosthesis, both including the 4-DOF socket joint developed in[19]. The models were pre-scaled to match the residual limb length ratio.

To scale the two models, a matching algorithm was developed (Fig. 4) to avoid error introduced by manual scaling of each model independently. The passive model was first scaled by manually altering the calibration model markers through the OpenSim GUI to best match actual marker placement, and then using the OpenSim scale tool. The tracking markers were then placed automatically via an optimization routine. Model marker positions were iteratively adjusted after performing an inverse kinematics (IK) analysis

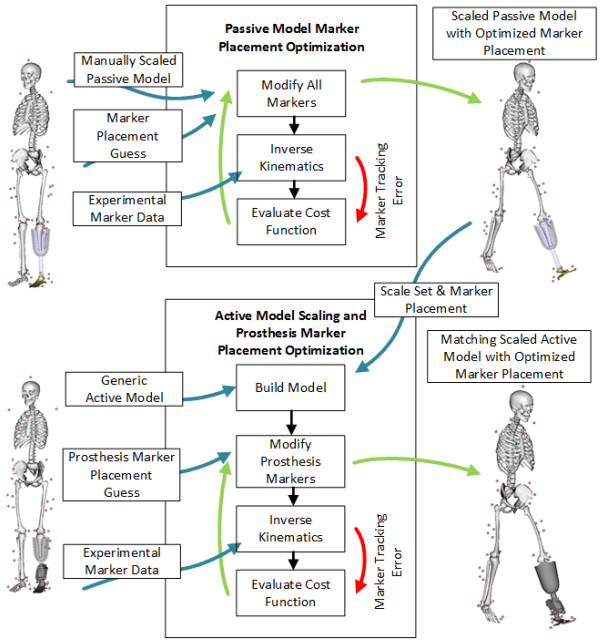

Fig. 4. The workflow of the model matching algorithm. After manually scaling a passive model, it is loaded in the script with a marker set placement guess and experimental marker data from a single walking trial. The first optimization loop minimizes marker error and prosthetic foot unloaded flexion by performing an inverse kinematics analysis and adjusting marker placement throughout the model with the exception of the sternum tracking marker. The second stage of the algorithm takes the scale set and optimized marker placements, and applies them to the generic active model. A second optimization loop then minimizes marker error on the prosthesis only since the rest of the model is identical to the passive model. After optimizing the marker placement with this method, average marker RMS for inverse kinematic analyses is about 5 mm.

with walking data through the MATLAB API, reducing the optimization cost C in (1). This function quantifies the sum of marker errors, which is the Euclidian norm of the vector from marker m experimental position $E(x,y,z)_m$ to model position $M(x,y,z)_m$ for each frame n of the IK results. A second term was added to minimize unloaded foot flexion *flex*, multiplied by a heuristically tuned weighting factor W. Tracking error RMS was minimized to 4.9 mm. Scale factors and marker placement from the passive model were then used to modify the active model. A similar optimization modified the prosthetic limb markers with the added penalty of the prosthesis actuator deviating from zero displacement on the first and last frames. This optimization reduced tracking error RMS to 5.7 mm. Tracking error RMS with manually placed markers is typically 10 mm or greater.

Post-processing of recorded data included calculating IK followed by inverse dynamics (ID) for all trials using OpenSim tools through the MATLAB API. COM trajectory was calculated, followed by joint power. Prosthesis power was estimated using the computed muscle control (CMC) tool since ID could not separate forces exactly in a closed loop kinematic chain. Pressure data were synchronized with motion data, averaged across sensor cells and filtered with a moving average window. Peak sensor pressure data were also filtered with a moving average filter. All datasets were averaged across trials, and standard deviations were calculated.

III. Results and Discussion

Results presented in this section highlight comparisons of walking mechanics when the test subject uses their daily use prosthesis and the experimental prototype with active alignment. In the following data presented, ESR represents data from the amputated limb using a passive energy storage and return prosthesis, and Intact ESR represents data from the contralateral intact limb. Similarly, AAP represents data from the amputated limb fitted with the active alignment prosthesis, and Intact AAP represents data from the intact contralateral limb from the same data set. All curves represent data averaged over the three trials.

Figure 5 presents the calculated IK generalized motions, ID generalized forces and power for the ankle, knee and hip joints in the sagittal plane. On the ankle plots, the prosthetic foot flexion coordinate is shown with intact ankle data (Fig. 5a) as commonly presented in the literature. Prosthetic foot mechanics in the AAP case represent the flex foot only, not including robotic ankle mechanics. In this figure, the kinematic data are shown in the top three plots. The main observations that can be taken from these three plots are that the prosthetic gait is very asymmetric in nature, and differences between passive and active trials throughout the body are subtle. The biggest differences are in the intact knee and hip joints (Figs. 5b and 5c), which are altered due to active alignment as found in earlier simulation studies [16]. Inspecting joint moments and powers, it is clear that there are

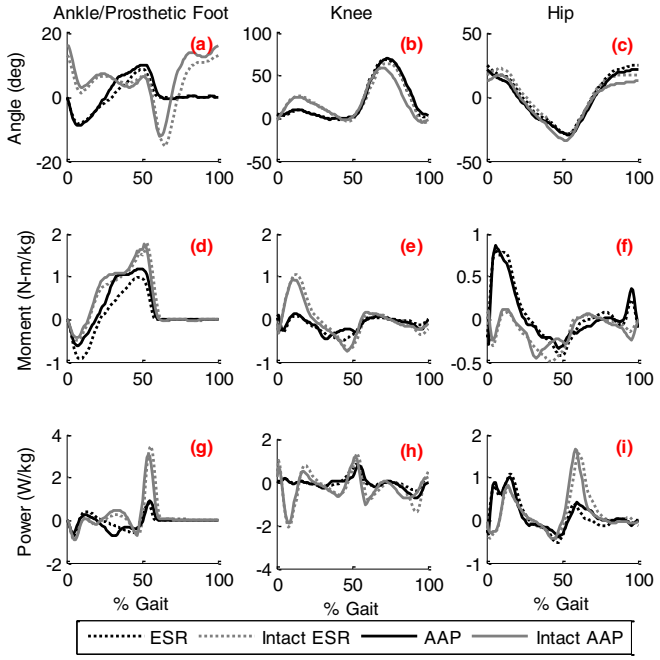

Fig. 5. Average sagittal plane biomechanics data for the ankle, knee and hip joints. ESR is data from the limb with amputation using a passive energy storage and return foot, and Intact ESR is data from the contralateral limb. AAP is data from the limb with amputation using the active alignment prosthesis, and Intact AAP is data from the contralateral limb. The data shown for the prosthetic foot in the AAP case only includes the passive foot attached to the active prosthesis.

no major changes to how the person is walking, and the added motions and forces of the active alignment ankle prosthesis introduce only small deviations from the user's normal gait pattern. The motion and force patterns are similar to gait data reported in the literature [20], [21].

Figure 6 shows average ground reaction force data from the experimental trials. It is seen on the prosthetic side that there is an increase in vertical force on heel strike and mid-stance when the prosthesis realigns the limb and lifts the subject (Fig. 6a). Peak horizontal ground reaction forces on the prosthetic side (Fig. 6c) are increased with the active prosthesis, indicating the subject is landing harder, and able to sustain support from the prosthesis slightly longer during roll-over. The intact right side shows little difference in peak values for horizontal and vertical forces, but shows less stance time on the active limb when using the active ankle prosthesis. Interestingly, the affected limb shows a longer stance percentage with the active ankle, which suggests that the active ankle reduces the loading demand on the residual limb, and normalizes gait symmetry in terms of stance percentage.

Figure 7 presents generalized motions, forces and powers for socket flexion/extension, and pistoning as introduced in [19], which are the two most clinically relevant coordinates in the socket joint. The most notable feature of these plots is the reduction of peak socket moments during late stance (Fig. 7c), as predicted in earlier simulation studies [16], which is associated with peak intra-socket pressures. Pistoning force resembles GRFs presented in (Fig. 6a) as expected, and near

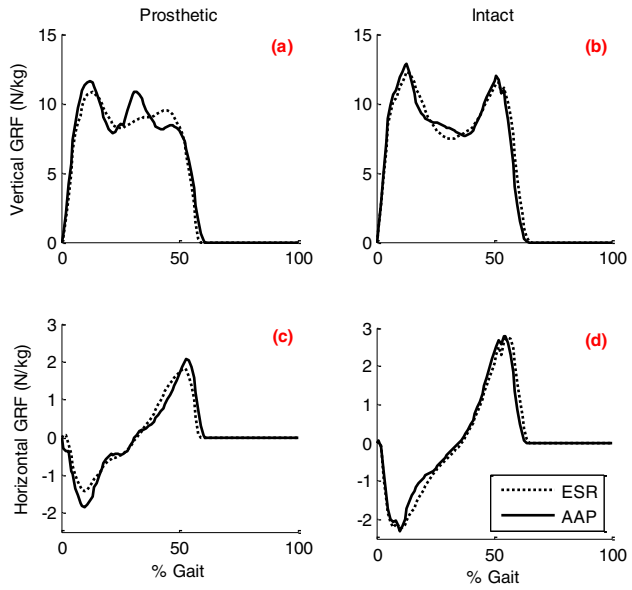

Fig. 6. Average normalized ground reaction forces are shown for trials where the test subject used the ESR foot prosthesis and AAP.

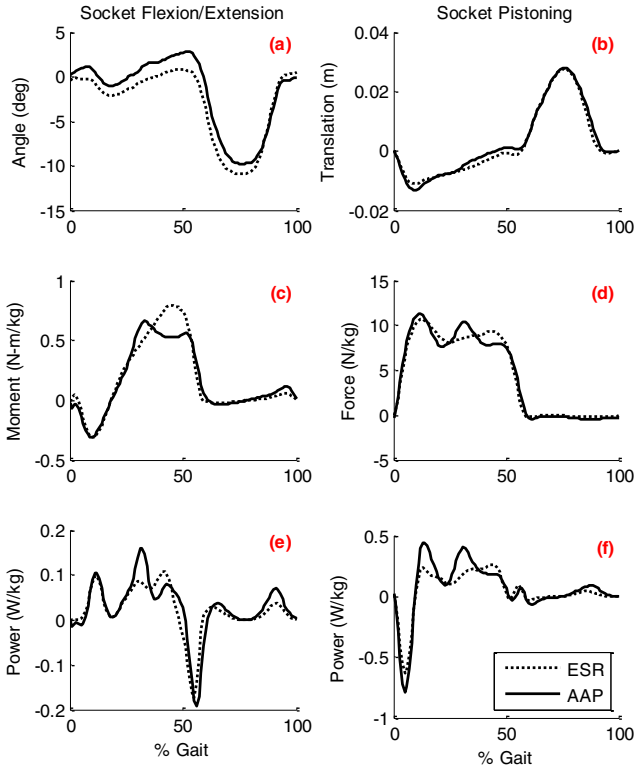

Fig. 7. Socket mechanics plots with average normalized sagittal plane generalized socket movement; forces and power are shown for trials where the test subject used the ESR foot prosthesis and AAP.

zero net power is generated throughout gait, which is expected of a passive joint.

The COM trajectories are shown in Fig. 8, zeroed with respect to the second peak seen during midstance of the intact contralateral limb. This allows for comparison of the COM trajectories, negating the effect that a heavier prosthesis will have on the center of mass as well as differences caused by

the alignment of prosthetic devices. It is observed that the active alignment prosthesis drops the center of mass lower after heel strike and before actuation, indicating the prosthesis height may not have been adjusted the same as the passive prosthesis height. The center of mass then peaks slightly higher with the active prosthesis, showing that the prototype is effectively injecting power during stance and performing net positive work to lift the subject.

In Fig. 9, the prototype prosthesis actuator mechanics are shown during gait. The top plot (Fig. 9a) displays the ball screw position, which quickly contracts to extend the prosthesis. The middle and lower plots present the prosthesis force and power. Force and power for the experimental prosthesis were estimated with the OpenSim CMC algorithm, which tracked the calculated IK results with a scaled model of the subject wearing the prosthesis prototype. This method was used to avoid problems encountered when applying standard ID methods to a closed kinematic chain, i.e. four-bar linkage with a linear actuator, which would result in false joint moments at every joint in the prosthesis where actuators do not exist. Calculations are a lumped sum of all force contributors in the prosthesis, including friction losses and static loading of the hard-stops. For this reason, the data that are shown for power can be considered prosthesis net power, which is positive during midstance.

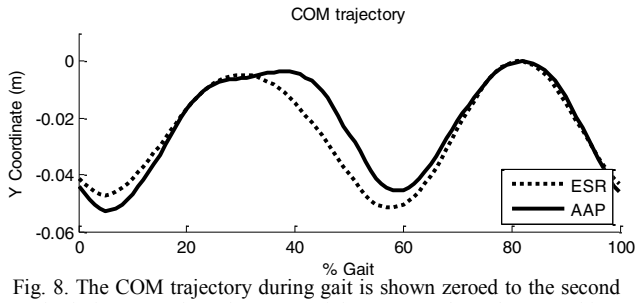

Fig. 8. The COM trajectory during gait is shown zeroed to the second peak, during contralateral stance. Trial averages where the test subject used the passive ESR foot prosthesis are represented by the dashed line, and trial averages from the AAP are represented by the solid line.

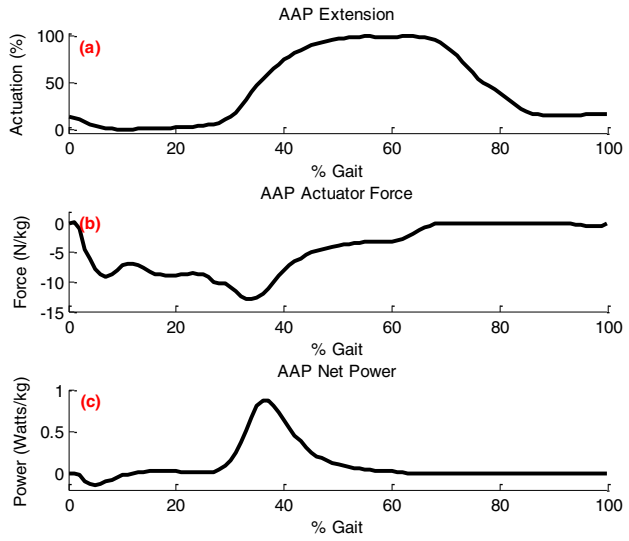

Fig. 9. Prosthesis, average extension, actuator force and power data are shown for the active alignment prosthesis.

Figure 10 shows average data recorded from the experimental prosthesis moment sensor when the prosthesis regulates a neutral position compared to employing active alignment. This data agrees with moments calculated for the residuum socket interface seen in Fig. 7c. The data in Fig. 11 is from pressure transducers on the tibial tubercle and residuum mid-posterior. These findings are perhaps the most clinically relevant. They show that both average (Fig. 11a) and peak (Fig. 11c) pressures on the tibial tubercle are decreased by over 10% when the active alignment prosthesis is used. Average pressure on the limb posterior increased during early stance following heel strike. However, peak pressures on the posterior are not increased.

Lastly, when the subject was asked to describe the level of effort and comfort experienced, they stated that it was easier to walk with the experimental device and that they felt

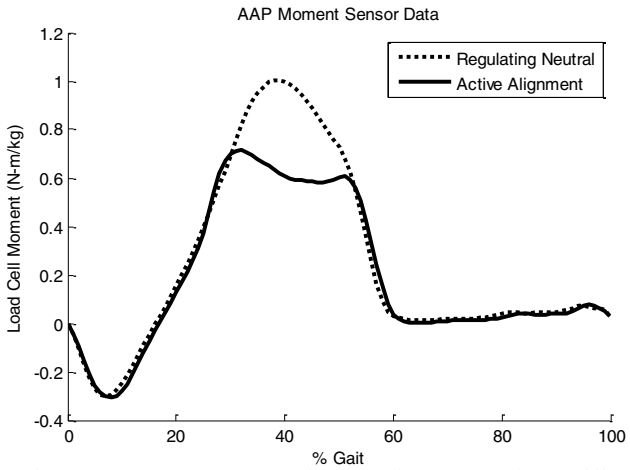

Fig.10. Average moment sensor data from five steps are shown while the experimental prosthesis regulates a neutral position, and employs active alignment.

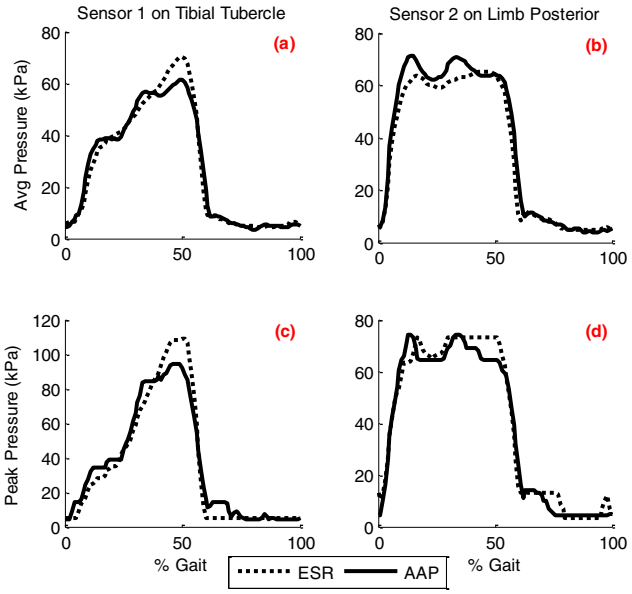

Fig. 11. Average and peak sensor array pressures are shown for the tibial tubercle region, and mid posterior region of the residual limb throughout the gait cycle.

they would have more endurance while walking on it. This is despite the device weighing more than twice that of their daily use device. They specifically said that it was less demanding on their residual limb and that the load bearing tissues felt less stressed.

IV. Conclusion

The findings in this paper provide evidence that altering foot-ankle prosthetic alignment during gait can reduce loading on the limb while injecting net positive power into the gait cycle. Peak pressures on the residual limb were reduced by over 10%. With minimal training, stance time increased on the affected limb and decreased on the healthy contralateral limb, providing a more symmetric gait. Additionally, the user's qualitative statement that it was easier to walk with the powered prosthesis than their passive ESR complemented the biomechanics results. Overall, the prosthesis did not fundamentally change or disrupt the subject's gait to achieve the intended pressure reduction on the residual limb. It is feasible that greater improvements would be seen if the subject were provided more time to adjust to the prosthesis, and with additional development of the controller and hardware. The reduced loading trend was consistent, and the approach merits further investigation and optimization.

Acknowledgment

This work was supported by a grant from the National Science Foundation (IIS-1526986) and by a grant from the National Center for Simulation in Rehabilitation Research.

References

[1] R. S. Gailey, K. E. Roach, E. B. Applegate, B. Cho, B. Cunniffe, S. Licht, M. Maguire, and M. S. Nash, "The Amputee Mobility Predictor: An instrument to assess determinants of the lower-limb amputee's ability to ambulate," *Arch. Phys. Med. Rehabil.*, vol. 83, no. 5, pp. 613–627, May 2002.

[2] J. E. Sanders, D. M. Bell, R. M. Okumura, and a J. Dralle, "Effects of alignment changes on stance phase pressures and shear stresses on transtibial amputees: measurements from 13 transducer sites.," *IEEE Trans. Rehabil. Eng.*, vol. 6, no. 1, pp. 21–31, Mar. 1998.

[3] H. a. M. Seelen, S. Anemaat, H. M. H. Janssen, and J. H. M. Deckers, "Effects of prosthesis alignment on pressure distribution at the stump/socket interface in transtibial amputees during unsupported stance and gait," *Clin. Rehabil.*, vol. 17, no. 7, pp. 787–796, Oct. 2003.

[4] H. C. Chadderton, "Prostheses, pain and sequelae of amputation, as seen by the amputee.," *Prosthet. Orthot. Int.*, vol. 2, pp. 12–14, 1978.

[5] A. R. Dillingham TR, "Use and Satisfaction with Prosthetic Devices Among Persons with Trauma-Related Amputations: A Long- Term Outcome Study," *Am. J. Phys. Med. Rehabil.*, vol. 80, no. 8, pp. 563–571, 2001.

[6] D. C. Norvell, J. M. Czerniecki, G. E. Reiber, C. Maynard, J. a Pecoraro, and N. S. Weiss, "The prevalence of knee pain and symptomatic knee osteoarthritis among veteran traumatic amputees and nonamputees.," *Arch. Phys. Med. Rehabil.*, vol. 86, no. 3, pp. 487–493, Mar. 2005.

[7] S. Portnoy, Z. Yizhar, N. Shabshin, Y. Itzchak, a Kristal, Y. Dotan-Marom, I. Siev-Ner, and a Gefen, "Internal mechanical conditions in the soft tissues of a residual limb of a trans-tibial amputee.," *J. Biomech.*, vol. 41, no. 9, pp. 1897–909, Jan. 2008.

[8] P. a. Struyf, C. M. van Heugten, M. W. Hitters, and R. J. Smeets, "The Prevalence of Osteoarthritis of the Intact Hip and Knee Among Traumatic Leg Amputees," *Arch. Phys. Med. Rehabil.*, vol. 90, no. 3, pp. 440–446, 2009.

[9] C. S. Hammarlund, M. Carlström, R. Melchior, and B. M. Persson, "Prevalence of back pain, its effect on functional ability and health-related quality of life in lower limb amputees secondary to trauma or tumour: a comparison across three levels of amputation," *Prosthet. Orthot. Int.*, vol. 35, no. 1, pp. 97–105, Mar. 2011.

[10] S. Bilodeau, R. Hébert, and J. Desrosiers, "Lower limb prosthesis utilisation by elderly amputees," *Prosthet. Orthot. Int.*, vol. 24, no. 2, pp. 126–132, Jan. 2000.

[11] C. E. Beekman and L. a Axtell, "Prosthetic use in elderly patients with dysvascular above-knee and through-knee amputations.," *Phys. Ther.*, vol. 67, no. 10, pp. 1510–6, Oct. 1987.

[12] R. L. Waters and S. Mulroy, "The energy expenditure of normal and pathologic gait," *Gait Posture*, vol. 9, no. 3, pp. 207–31, Jul. 1999.

[13] S. D'Andrea, N. Wilhelm, A. K. Silverman, and A. M. Grabowski, "Does Use of a Powered Ankle-foot Prosthesis Restore Whole-body Angular Momentum During Walking at Different Speeds?," *Clin. Orthop. Relat. Res.*, vol. 472, no. 10, pp. 3044–54, Oct. 2014.

[14] A. K. LaPrè and F. Sup, "Non-Anthropomorphic Ankle Prosthesis Design, Redefining ankle mechanics to better suit amputee needs," *IEEE Int. Conf. Rehabil. Robot.*, p. in press, 2013.

[15] A. K. LaPre and F. Sup, "Redefining Prosthetic Ankle Mechanics," in *IEEE International Conference on Rehabilitation Robotics*, 2013.

[16] A. K. LaPre, B. R. Umberger, and F. Sup, "Simulation of a Powered Ankle Prosthesis with Dynamic Joint Alignment," in *Proc. - IEEE Int. Conf. Engineering in Medicine and Biology Society*, 2014, pp. 1618–1621.

[17] A. K. LaPre and F. Sup, "A Control Strategy for an Active Alignment Transtibial Prosthesis," in *ASME 2015 Dynamic Systems and Control Conference*, 2015, p. V001T18A005.

[18] A. K. LaPre, B. R. Umberger, and F. C. Sup IV, "A Robotic Ankle Prosthesis with Dynamic Alignment," *J. Med. Device.*, vol. 10, no. c, pp. 1–9, 2016.

[19] A. K. LaPre, "A Lower Limb Prosthesis With Active Alignment for Reduced Limb Loading," University of Masachusetts Amherst, 2016.

[20] D. A. Winter and S. E. Sienko, "Biomechanics of below-knee amputee gait," *J. Biomech.*, vol. 21, no. 5, pp. 361–367, 1988.

[21] M. P. E. Sanderson, David J., "Lower Extremity Kinematic and Kinetic Adaptions in Unilateral Below-Knee Amputees During Walking.pdf," *Gait Posture*, vol. 6, pp. 126–136, 1997.